Indicators of Gas Source Proximity using Metal Oxide Sensors in a Turbulent Environment

Achim J. Lilienthal, Tom Duckett
Örebro University
Dept. of Technology, AASS
S-70182 Örebro, Sweden
achim@lilienthals.de,
tom.duckett@tech.oru.se

Hiroshi Ishida
Tokyo Univ. of Agriculture & Technology
Dept. of Mechanical Systems Engineering
Tokyo, Japan
h_ishida@cc.tuat.ac.jp

Felix Werner
University of Tübingen
Wilhelm-Schickard Institute
D-72076 Tübingen, Germany
fwerner@informatik.uni-tuebingen.de

***Abstract*— This paper addresses the problem of estimating proximity to a gas source using concentration measurements. In particular, we consider the problem of gas source declaration by a mobile robot equipped with metal oxide sensors in a turbulent indoor environment. While previous work has shown that machine learning classifiers can be trained to detect close proximity to a gas source, it is difficult to interpret the learned models. This paper investigates possible underlying indicators of gas source proximity, comparing three different statistics derived from the sensor measurements of the robot. A correlation analysis of 1056 trials showed that response variance (measured as standard deviation) was a better indicator than average response. An improved result was obtained when the standard deviation was normalized to the average response for each trial, a strategy that also reduces calibration problems.**

***Index Terms*— mobile nose; gas source localisation; turbulent gas distribution.**

I. Introduction

Traditionally, most work on gas source localisation by mobile robots has concentrated on the sub-task of *gas source tracing*, which is the problem of determining a path towards a distant gas source. If information about the local wind vector is available, the upwind direction can be used as an indicator of the direction to the source. Thus, many successful implementations of gas source tracing strategies combine a gas searching behaviour with periods of upwind movement [5], [13], [2], [12]. So far, the corresponding experiments were all carried out in environments with a strong uniform airflow (generated externally). A strong airflow was needed because of the detection limits of the wind measuring devices used, which were not low enough to measure the weak air currents that are typically encountered in industrial or domestic buildings [4], [11]. With a faster speed of the robot, it would also become increasingly difficult to isolate a small airspeed vector from the ground speed vector of the robot [6]. Another problem for an anemotactic gas source tracing strategy is that in cases where the wind direction is not uniform, upwind searching can be misled by the unstable wind field in regions where different air currents mix together. This was observed by Ishida et al. in experiments in a clean room with two air supply openings [3].

Since a gas source tracing strategy requires only to estimate the direction toward a gas source, a further sub-task is to decide whether the source has actually been found. *Gas source declaration* is the problem of determining the certainty that a source has been located based on concentration measurements (possibly in combination with other sensor modalities, an aspect not addressed here).

This paper addresses the problem of gas source declaration using only metal oxide sensors in a turbulent indoor environment, without an artificially created airflow. Metal oxide sensors comprise a heating element coated with a sintered semiconducting material. The measured quantity is the resistance R_S of the surface layer at an operating temperature of 300°C to 500°C [1]. Exposed to a reducing gas, the potential barrier at the grain boundary is lowered, and thus the resistance of the surface layer decreases. In consequence of the measurement principle, metal oxide sensors have some drawbacks, including low selectivity, and a comparatively high power consumption (caused by the heating device). Furthermore, metal oxide sensors are subject to a long response time and an even longer decay time. However, this type of gas sensor is most often used for experiments in mobile robot olfaction because it is inexpensive, highly sensitive and relatively unaffected by changing environmental conditions such as room temperature or humidity.

A previous work [9], [8] introduced a gas source declaration strategy based on classification of gas sensor readings using machine learning classifiers (support vector machines and artificial neural networks). A mobile robot equipped with metal oxide gas sensors performed a rotation manoeuvre at a given location facing an evaporating gas source (see Fig. 1), and then used the recorded sensor readings to classify whether the distance of the robot from the source was below a given threshold. The results showed that support vector machines were able to learn to discriminate between positive and negative examples of a nearby gas source with a classification rate between 65.9% and 97.1%, depending on the given distance between positive and negative examples (from 40 cm to 100 cm) [7].

However, despite the success of this approach, one problem with machine learning classifiers such as support vector machines is that it can be very difficult to interpret the learned models. In this paper, we try to understand the possible underlying indicators of gas source proximity

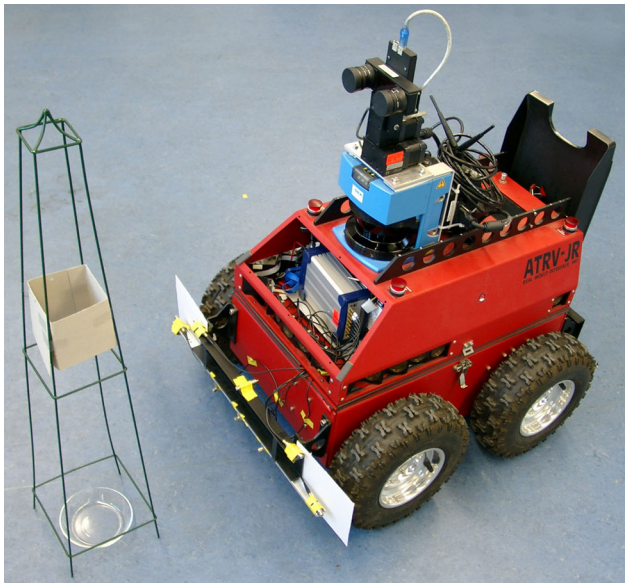

Fig. 1. The gas-sensitive mobile robot Arthur in front of the gas source. The position of the robot in the image corresponds to the starting position in a trial with minimum distance to the gas source, i.e. a trial where the robot just avoids to push over the bowl that served as a gas source.

using exactly the same experimental set-up as in the previous work [9], [8]. We compare three different indicators of gas source proximity, in particular, concerning the average sensor response versus the variance of the sensor response, i.e., the magnitude of fluctuations in the signal. In order to allow for a direct comparison, the variance of the sensor response is measured as the standard deviation of the sensor measurements, thus having the same units as the average response. (So, whenever we refer to the response variance in this paper, it is implicitly understood that it is measured as the standard deviation.) A correlation analysis of 1056 trials, where the mobile robot recorded gas sensor measurements at several distances from the source, showed that the response variance was a better indicator of the distance to the gas source than the average response. A slightly better result was obtained when the standard deviation was normalized to the average response for each trial, a strategy that also reduces calibration problems.

II. Experimental Set-Up

A. Robot

The gas sensor measurements were carried out at Tübingen University with the mobile robot "Arthur" (length = 80 cm, width = 65 cm, height without laser range scanner = 55 cm), ATRV-Jr from iRobot (see Fig. 1). Apart from the gas sensors, only odometry and the data from the SICK laser were utilised for the experiments presented here to determine the position of the robot.

B. Gas Sensors

The gas sensing system is based on the commercially available device VOCmeter-Vario (AppliedSensor), which is described in detail in [10]. For the experiments presented in this paper, seven metal oxide sensors were placed on the robot as shown in Fig. 2. Five TGS 2620 sensors were mounted symmetrically at a height of 9 cm above the floor on the front bumper of the robot, and two additional sensors of type TGS 2600 were mounted at a height of 16 cm above the floor. The distance of the lower sensors to the middle of the bumper was 0 cm, $\pm$16 cm, and $\pm$40 cm, while the upper sensors were mounted at a distance of $\pm$32 cm to the centre (see Fig. 2). The distance between the outer sensors and the front wheels was very small. In order to avoid a corruption of the results due to an additional airflow created by the wheels, a shield made of cardboard was placed inbetween the wheels and the sensors.

C. Procedure

All experiments were carried out in a 15.4 m $\times$ 5.1 m laboratory room. A floor plan is shown in Fig. 3, including doors, windows, cupboards and desks. In addition, the tested gas source positions are indicated by circles. A total of N = 1056 trials were performed using three different source locations and four different orientations with respect to the source as indicated in Fig. 3. For each source position, 176 trials were carried out at a distance d directly in front of the gas source ($d = d_0$), i.e. at the minimum possible distance between robot and source, alternating with 176 trials at a randomly chosen larger distance of $d = d_0 + \Delta d$ with Δd = 5 cm, 10 cm, 15 cm, 20 cm, 25 cm, 30 cm, 40 cm, 50 cm, 60 cm, 80 cm and 100 cm, respectively. After each trial, the robot was stopped for 60 s in order to avoid disturbance from the preceding measurements due to the long decay time of the sensors. All the robot positions tested are shown in Fig. 3 for the rightmost source position, using triangles that indicate the centre of the robot and its initial heading.

D. Environment and Gas Source

In order to investigate the problem of gas source declaration under real world conditions, an unmodified indoor environment was chosen for this investigation. The room was not ventilated and up to two persons were working,

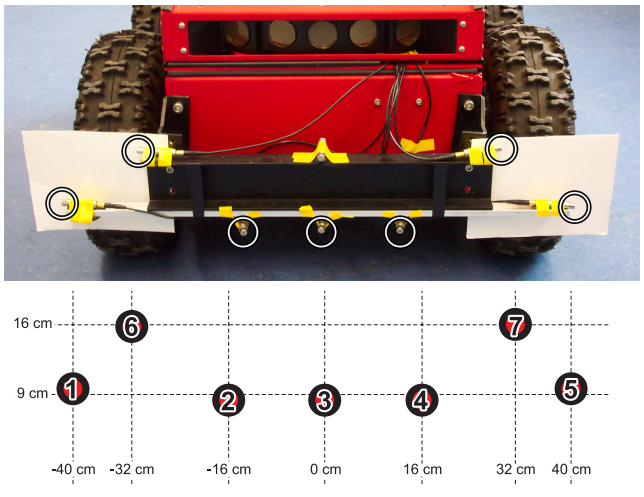

Fig. 2. Setup of the gas sensor array.

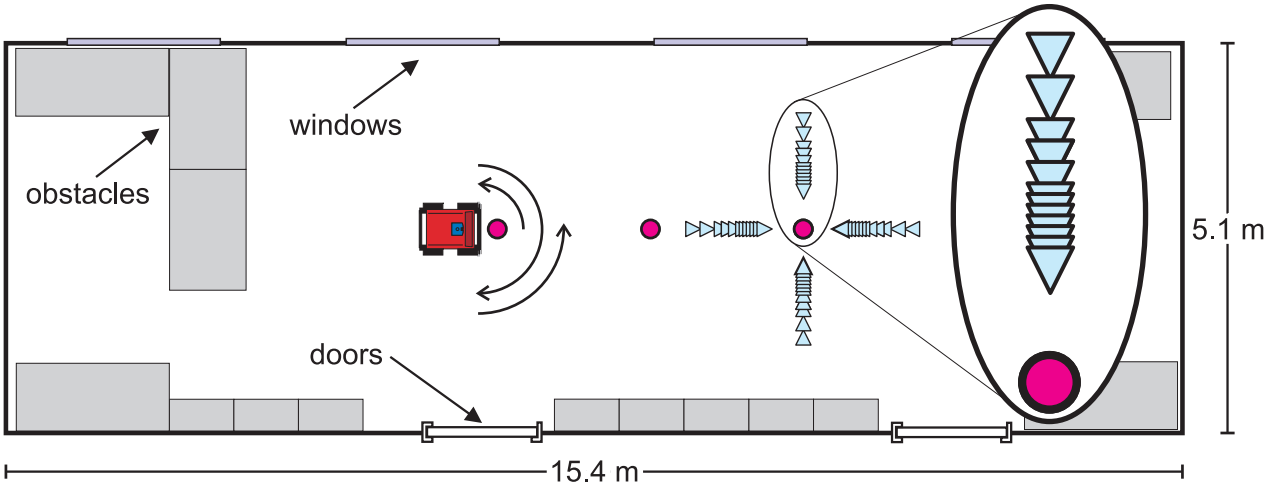

Fig. 3. Floor plan of the laboratory room in which the experiments described in Section II were performed. Indicated are the windows at the upper and the doors at the lower side as well as the obstacles in the room (cupboards and desks). The tested locations of the gas source are indicated by circles. The mobile robot is sketched in the start position of a trial with minimum possible distance to the gas source, and the rotation maneouvre carried out by the robot is indicated by three arrows. All of the tested robot positions are shown for the rightmost source location, using triangles that indicate the centre of the robot and its initial heading.

moving and sometimes leaving or entering the room during the experiments. Although the windows were kept closed and the persons were told to be careful, this indoor environment can be considered as uncontrolled to some extent.

The gas source was a bowl with a diameter of 140 mm and a height of 20 mm filled with Single Malt Whiskey (40% alcohol), which was used because it is non-toxic, less volatile than pure ethanol and easily detectable by metal oxide sensors. In order to be detected by the laser range scanner, a frame made of wire with a cardboard marking mounted on top was placed above the container (see Fig. 1).

E. Data Recording Startegy

Bearing in mind the task of gas source declaration and the properties of gas distribution in real world environments, a data recording strategy was chosen that provides temporally as well as spatially sampled concentration data. The gas sensor readings were acquired while the robot performed a rotation manoeuvre consisting of three successive rotations: 90° to the left, 180° to the right (without stopping) and finally 90° to the left again (see Fig. 3). Initially, the robot was oriented towards the gas source. The rotation was performed with an angular speed set to 4°/s corresponding to a total time of 90 s to complete the manoeuvre. Simultaneously, sensor readings were acquired at a rate of 4 Hz.

III. Data Processing

A. Data Pre-Processing

Since the number of readings per trial varied slightly, the measurements of each trial i were converted to a response vector $\vec{R}^{(i)}$ with dimension N_R = 361 by linear interpolation. This corresponds to rotation steps of 1°.

B. Indicators of Gas Source Proximity

For the correlation analysis presented in Section IV, we consider three different indicators, which can be calculated from the response vector $\vec{R}^{(i)}$ of a particular trial.

In the case of a smooth, radially symmetric concentration gradient with a maximum at the source location, the average sensor response $\mu^{(i)}$ during trial i would monotonically decrease with increasing distance from the gas source, and thus would provide a perfect indication of the distance to the source. The first indicator investigated here is therefore the average over the N_R values of the response vector $R_j^{(i)}$ of a particular trial i, calculated as

$$\mu^{(i)} = \frac{1}{N_R} \sum_{j=1}^{N_R} R_j^{(i)}. \tag{1}$$

The second indicator investigated is the response variance, measured as the response standard deviation in a particular trial i, calculated as

$$\sigma^{(i)} = \sqrt{\frac{1}{N_R - 1} \sum_{j=1}^{N_R} (R_j^{(i)} - \mu^{(i)})^2}. \tag{2}$$

Finally, the normalised standard deviation $\hat{\sigma}^{(i)}$, calculated by dividing the standard deviation by the average response for a particular trial i was also investigated as a dimensionless indicator:

$$\hat{\sigma}^{(i)} = \sigma^{(i)} / \mu^{(i)}. \tag{3}$$

IV. Results

The profile of the raw measurements does not reveal the distance to the gas source in a straightforward way. This can be seen in Fig. 5, which shows the response vectors for sensor 3 (the middle sensor in the lower row, see Fig. 2) in four trials carried out at different distances from the gas source. Since the robot carries out a rotation

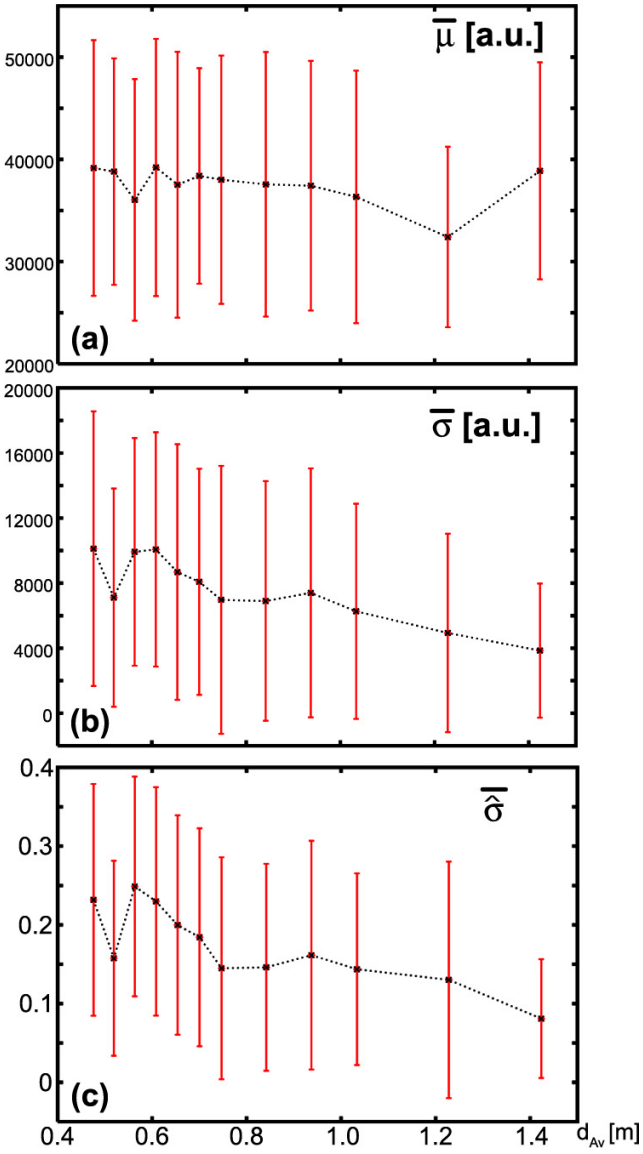

Fig. 4. Comparison of (a) average trial response, (b) standard deviation during a trial, and (c) standard deviation divided by the average trial response, all measured against the average distance to the gas source d_{Av}. Each figure shows the average of the respective indicator over the trials with a particular distance from the gas source. The respective standard deviation is indicated by error bars.

maneouvre, the distance between the sensors and the gas source changes during collection of the sensor measurements. The indicators derived for each trial are therefore assigned to the average distance d_{Av} of a respective sensor during the rotation maneouvre. Trial #354, for example, which is one of the trials shown in Fig. 5, corresponds to an average distance of d_{Av} = 47.6 cm. In this case, the distance between the considered sensor 3 and the centre of the gas source is 25 cm at the beginning and at the end of the trial, and the maximum distance from the gas source is 76.3 cm at the points where the robot reverses its rotation.

Under the given conditions, a dependency between the average sensor response $\mu^{(i)}$ (as defined in Eq. 1) and the average distance from the source during this trial $d_{Av}^{(i)}$ could not be observed. Fig. 4(a) shows for each of the 12 different distances, at which trials were carried out, the average of the average response values, calculated as

$$\overline{\mu}(d_{Av}) = \frac{1}{|S(d_{Av})|} \sum_{i \in S(d_{Av})} \mu^{(i)}, \tag{4}$$

and the respective standard deviation, calculated as

$$\sigma_{\mu}(d_{Av}) = \sqrt{\frac{1}{|S(d_{Av})|-1} \sum_{i \in S(d_{Av})} (\mu^{(i)} - \overline{\mu})^2}. \tag{5}$$

Note that the sum in Eq. 4 and Eq. 5 runs over the set $S(d_{Av})$ of all trials with a particular average distance from the gas source, and that $|S(d_{Av})|$ denotes the number of trials in the respective set.

The fact that a decreasing average concentration could not be established with our setup is reflected by the linear correlation coefficient $r_{\mu,d_{Av}}$ between the average sensor response μ and the average distance d_{Av} during a trial, which was close to zero for all sensors (-0.08 for sensor 3). The linear correlation coefficients for all sensors are given in Table I. For a particular indicator quantity x, the linear correlation coefficient with the average distance d_{Av} was calculated as

$$r_{x,d_{Av}} = \frac{cov_{x,d_{Av}}}{\sigma_x \cdot \sigma_{d_{Av}}} \tag{6}$$

with

$$cov_{x,d_{Av}} = \frac{1}{N-1} \sum_{i=1}^{N} (x^{(i)} - \overline{x})(d_{Av}^{(i)} - \overline{d_{Av}}), \tag{7}$$

$$\sigma_{x|d_{Av}} = \sqrt{\frac{1}{N-1} \sum_{i=1}^{N} (x^{(i)}|d_{Av}^{(i)} - \overline{x}|\overline{d_{Av}})^2}. \tag{8}$$

Here, N denotes the total number of trials, i.e. N = 1056 in this paper.

Looking at the standard deviation $\sigma^{(i)}$ of the sensor response in individual trials (as defined in Eq. 2), rather than the response average, reveals a different picture. Fig. 4(b) shows the progression of the average of this indicator, which was calculated according to Eq. 4 as

$$\overline{\sigma}(d_{Av}) = \frac{1}{|S(d_{Av})|} \sum_{i \in S(d_{Av})} \sigma^{(i)}. \tag{9}$$

As can be seen from the plot, this parameter tends to decrease with increasing distance from the gas source, indicated by a linear correlation coefficient of -0.22 for sensor 3.

A slightly stronger correlation, indicated by a linear correlation coefficient of -0.28 for sensor 3, was found using the normalised standard deviation $\hat{\sigma}^{(i)}$, as defined in Eq. 3. Fig. 4(c) shows the progression of the average of this indicator, calculated as

$$\overline{\hat{\sigma}}(d_{Av}) = \frac{1}{|S(d_{Av})|} \sum_{i \in S(d_{Av})} \hat{\sigma}^{(i)}. \tag{10}$$

Linear correlation coefficients for the three indicators introduced in this section are given in Table I for all seven

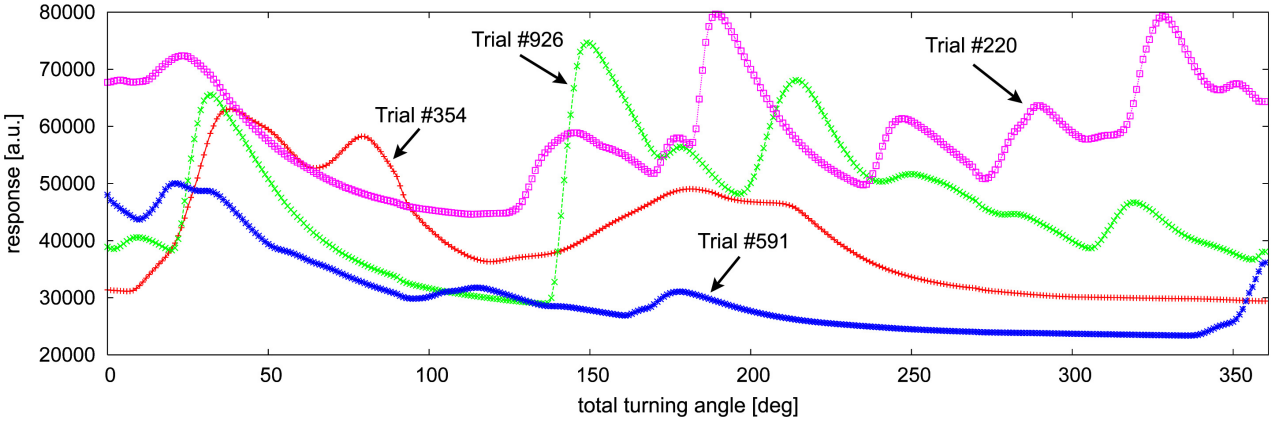

Fig. 5. Examples of the profile of the response vector $\vec{R}^{(i)}$ calculated from data recorded with sensor 3 in four trials: i = 354 (d_{Av} = 47.6 cm), i = 926 (d_{Av} = 70.0 cm), i = 591 (d_{Av} = 93.7 cm), and i = 220 (d_{Av} = 142.4 cm).

gas sensors used. Each of these indicators summarises 1056 trials with a total of approx. 380000 measurements. The general trend – almost no correlation of the response average, a moderate correlation of the response standard deviation, and a slightly stronger correlation of the normalised response standard deviation – could be observed for all seven sensors. A second general observation is a stronger correlation for the sensors in the lower row (sensor 1 - 5) compared to the sensors in the upper row (sensor 6, 7). Due to the very similar response to alcoholic substances of the TGS 2600 gas sensors (used in the upper row) and the TGS 2620 sensors (used in the lower row), this observation could be attributed to the fact that ethanol, which is heavier than air, tends to stay near the floor and thus, the measurements of higher sensors contain less information in the case of a ground level gas source. Another possible reason could be that the orientation of the gas sensors was different for sensors 3, 4, and 5, which were oriented towards the gas source at the beginning of the rotation maneouvre, and sensors 1, 5, 6, and 7, which were oriented perpendicular to the gas source at the beginning of the rotation maneouvre.

V. Further Evidence from LIF Measurements

In the experiment discussed above, the strength of the fluctuations of the sensor signal provided a better indication of proximity to a gas source than the average response. This finding is supported by direct investigations on the structure of a turbulent plume. We refer to laser-induced fluorescence (LIF) measurements of the structure of a turbulent water plume here, because we could not identify publications that explicitly address the course of the concentration variance in a turbulent aerial plume. It is, however, not straightforward to transfer the results of underwater experiments to the condition of a different fluid (air) even if similar flow velocities and source characteristics are considered. The turbulent intensity is far smaller, and diffusion is much slower in water than in air. Because the scaling factor for the Reynolds number is different from the scaling factor for the diffusion rate, it is also not possible to scale the flow field in order to match both the Reynolds number and the diffusion rate. However, the qualitative properties of the concentration distribution should be similar in air and in water. Generally, the analyte released from the source is advected downstream while turbulent fluctuations stir and spread the filaments, resulting in filaments with a high concentration of the analyte, interspersed with regions where the analyte concentration is effectively zero.

	Sensor						
Indicator	1	2	3	4	5	6	7
$r_{\mu,d_{Av}}$	-0.030	-0.075	-0.080	-0.087	-0.034	-0.004	0.002
$r_{\sigma,d_{Av}}$	-0.227	-0.226	-0.224	-0.225	-0.186	-0.158	-0.160
$r_{\hat{\sigma},d_{Av}}$	-0.259	-0.289	-0.280	-0.284	-0.228	-0.216	-0.225

TABLE I

Linear correlation coefficients for the indicators μ, σ, and $\hat{\sigma}$, as defined in Eqs. 1, 2, and 3.

The course of the concentration variance in a turbulent chemical plume was investigated by Webster et al. [15] using laser-induced fluorescence measurements (LIF), which provide a non-intrusive way to measure the instantaneous spatial concentration distribution. Vertical concentration profiles were recorded over 600 s on the plume centreline at a distance of 20, 40, 60, and 80 cm from the source. A comparison of the vertical profiles of the time-averaged concentration with the vertical profiles of the concentration variance showed that the variance decreased faster with increasing distance from the source than the time-averaged concentration. The plume became homogeneous faster than it diluted due to turbulent mixing and the effect of diffusion acting on the steep gradients created by turbulent stirring. Bearing in mind the difficulties of transferring this result strictly to the conditions considered in the mobile robot experiments described in this paper, the LIF measurements by Webster et al. nevertheless provide evidence that the magnitude of concentration fluctuations can provide a more reliable indicator of proximity to a gas source than the absolute concentration.

VI. Conclusions

This paper presents a correlation analysis of metal oxide gas sensor measurements recorded with a mobile robot

during a rotation maneouvre at different distances from a gas source. The analysis of 1056 trials, with a duration of 90 s each, showed that the strength of the fluctuations of the sensor signal (measured as the response standard deviation over a trial) provided a better indication of proximity to a gas source than the average response. This finding is supported by a discussion of previous results from laser-induced fluorescence measurements of turbulent underwater plumes, which showed that the magnitude of the concentration fluctuations exhibited a steeper gradient along the downstream direction than the average concentration [15].

It has to be noted that it is not straightforward to draw general conclusions from the experimental results presented in Section IV. The gas sensor readings do not reflect the odour landscape in a one-to-one manner. First, the metal oxide sensors used do not adapt quickly to concentration changes, which essentially limits their bandwidth. Individual patches of high concentration, for example, can only be distinguished in the received signal if they are sufficiently separated. Otherwise they would appear as a single peak. The variance (or standard deviation) in the sensor response therefore reflects the concentration fluctuation at the locations the sensor was exposed to but also whether patches of analyte gas tend to be well separated or occur in clusters.

Another effect that has to be taken into account is the interaction of the robot body with the gas distribution. Currently, it is not possible to decide from our data whether the movement of the robot increases or decreases discrimination of distances to the gas source, or whether this effect can be disregarded here.

All three indicators considered in Section IV exhibit pronounced variations, indicated by the relatively long error bars in Fig. 4. This is mainly a consequence of the intention to find an indication of gas source proximity that does not depend on the upwind direction. The experiment described in Section II includes an equal number of trials from four directions with respect to the gas source. Assuming a non-negligible influence of advective transport, as is typical even in an indoor environment without ventilation due to the fact that weak air currents exist as a result of pressure (draught) and temperature inhomogeneities (convection flow) [14], the average concentration field takes a plume shape. Thus, the received sensor response is expected to vary largely with the orientation of the robot. It is of particular note that despite the large variations of the signal with respect to the direction of a particular trial, the response variance was nevertheless found to provide a reasonable indication of proximity to the gas source.

The response variance was measured as the standard deviation over a trial. A slightly stronger correlation with the distance from the gas source was found when the normalised standard deviation, i.e. the standard deviation divided by the response average, was used instead. Using the normalised standard deviation has the further advantage that it mitigates problems like the dependency on changing environmental conditions (temperature, humidity) or calibration issues when different sensors are to be compared.

Further investigations should address the possibility of using the response variance gradient in the context of a gas source tracing strategy. Since only distances of up to approx. 1.5 m from the gas source were considered in the experiments presented in this paper, further investigations would also be desirable to determine the range where the gradient of the response variance is strong enough to be used for gas source tracing, and especially whether the average response might provide a better indication at larger distances from the source.

REFERENCES

[1] Julian W. Gardner and Philip N. Bartlett. *Electronic Noses - Principles and Applications*. Oxford Science Publications, Oxford, 1999.

[2] A.T. Hayes, A. Martinoli, and R.M. Goodman. Distributed Odor Source Localization. *IEEE Sensors Journal, Special Issue on Electronic Nose Technologies*, 2(3):260–273, 2002. June.

[3] Hiroshi Ishida, Yukihiko Kagawa, Takamichi Nakamoto, and Toyosaka Moriizumi. Odour-Source Localization in the Clean Room by an Autonomous Mobile Sensing System. *Sensors and Actuators B*, 33:115–121, 1996.

[4] Hiroshi Ishida, Takamichi Nakamoto, Toyosaka Moriizumi, Timo Kikas, and Jiri Janata. Plume-Tracking Robots: A New Application of Chemical Sensors. *Biol. Bull.*, 200:222–226, April 2001.

[5] Hiroshi Ishida, K. Suetsugu, Takamichi Nakamoto, and Toyosaka Moriizumi. Study of Autonomous Mobile Sensing System for Localization of Odor Source Using Gas Sensors and Anemometric Sensors. *Sensors and Actuators A*, 45:153–157, 1994.

[6] Hiroshi Ishida, Minjie Zhu, Ken Johansson, and Toyosaka Moriizumi. Three-Dimensional Gas/Odor Plume Tracking with Blimp. In *Proceedings of the International Conference on Electrical Engineering 2004 (ICEE 2004)*, pages 117–120, Sapporo, Japan, 2004.

[7] Achim Lilienthal. *Gas Distribution Mapping and Gas Source Localisation with a Mobile Robot*. PhD thesis, Wilhelm-Schickard Institute, University of Tübingen, 2004.

[8] Achim Lilienthal, Holger Ulmer, Holger Fröhlich, Andreas Stützle, Felix Werner, and Andreas Zell. Gas Source Declaration with a Mobile Robot. In *Proceedings of the IEEE International Conference on Robotics and Automation (ICRA 2004)*, pages 1430–1435, 2004.

[9] Achim Lilienthal, Holger Ulmer, Holger Fröhlich, Felix Werner, and Andreas Zell. Learning to Detect Proximity to a Gas Source with a Mobile Robot. In *Proceedings of the IEEE/RSJ International Conference on Intelligent Robots and Systems (IROS 2004)*, pages 1444–1449, 2004.

[10] Achim Lilienthal, Andreas Zell, Michael R. Wandel, and Udo Weimar. Sensing Odour Sources in Indoor Environments Without a Constant Airflow by a Mobile Robot. In *Proceedings of the IEEE International Conference on Robotics and Automation (ICRA 2001)*, pages 4005–4010, 2001.

[11] M. Pluijm, G. Sars, and C. H. Massen. Calibration Unit for Micro-Anemometers at Very Low Air Velocities. *Appl. Sci. Res.*, 43:227–234, 1986.

[12] R. A. Russell, Alireza Bab-Hadiashar, Rod L. Shepherd, and Gordon G. Wallace. A Comparison of Reactive Chemotaxis Algorithms. *Robotics and Autonomous Systems*, 45:83–97, 2003.

[13] R. Andrew Russell, David Thiel, Reimundo Deveza, and Alan Mackay-Sim. A Robotic System to Locate Hazardous Chemical Leaks. In *Proceedings of the IEEE/RSJ International Conference on Intelligent Robots and Systems (IROS 1995)*, pages 556–561, 1995.

[14] Michael R. Wandel, Achim Lilienthal, Tom Duckett, Udo Weimar, and Andreas Zell. Gas Distribution in Unventilated Indoor Environments Inspected by a Mobile Robot. In *Proc. of the IEEE Int. Conference on Advanced Robotics (ICAR 2003)*, pages 507–512, 2003.

[15] D. R. Webster, S. Rahman, and L. P. Dasi. Laser-Induced Fluorescence Measurements of a Turbulent Plume. *Journal of Engineering Mechanics*, 129:1130–1137, October 2003.